Interplay of Mg^{2+}, ADP, and ATP in the cytosol and mitochondria: Unravelling the role of Mg^{2+} in cell respiration

Elisabeth Gout, Fabrice Rébeillé, Roland Douce, and Richard Bligny[1]

Laboratoire de Physiologie Cellulaire & Végétale, Institut de Recherches en Technologies et Sciences pour le Vivant, Commissariat à l'Energie Atomique et aux Energies Alternatives (CEA), Unité Mixte de Recherche 5168 CNRS, Université Grenoble Alpes (UGA), Institut National de la Recherche Agronomique (INRA), CEA, F-38054 Grenoble, France

Edited by George H. Lorimer, University of Maryland, College Park, MD, and approved September 19, 2014 (received for review April 7, 2014)

In animal and plant cells, the ATP/ADP ratio and/or energy charge are generally considered key parameters regulating metabolism and respiration. The major alternative issue of whether the cytosolic and mitochondrial concentrations of ADP and ATP directly mediate cell respiration remains unclear, however. In addition, because only free nucleotides are exchanged by the mitochondrial ADP/ATP carrier, whereas MgADP is the substrate of ATP synthase (EC 3.6.3.14), the cytosolic and mitochondrial Mg^{2+} concentrations must be considered as well. Here we developed in vivo/in vitro techniques using ^{31}P-NMR spectroscopy to simultaneously measure these key components in subcellular compartments. We show that heterotrophic sycamore (*Acer pseudoplatanus* L.) cells incubated in various nutrient media contain low, stable cytosolic ADP and Mg^{2+} concentrations, unlike ATP. ADP is mainly free in the cytosol, but complexed by Mg^{2+} in the mitochondrial matrix, where [Mg^{2+}] is tenfold higher. In contrast, owing to a much higher affinity for Mg^{2+}, ATP is mostly complexed by Mg^{2+} in both compartments. Mg^{2+} starvation used to alter cytosolic and mitochondrial [Mg^{2+}] reversibly increases free nucleotide concentration in the cytosol and matrix, enhances ADP at the expense of ATP, decreases coupled respiration, and stops cell growth. We conclude that the cytosolic ADP concentration, and not ATP, ATP/ADP ratio, or energy charge, controls the respiration of plant cells. The Mg^{2+} concentration, remarkably constant and low in the cytosol and tenfold higher in the matrix, mediates ADP/ATP exchange between the cytosol and matrix, [MgADP]-dependent mitochondrial ATP synthase activity, and cytosolic free ADP homeostasis.

plant cell respiration | ADP and Mg^{2+} homeostasis | cytosolic free ADP | cytosolic free Mg^{2+} | ^{31}P-NMR spectroscopy

In heterotrophic and well-oxygenated plant cells, ATP is regenerated from ADP principally by glycolysis and mitochondrial oxidative phosphorylation. Surprisingly, although ATP synthesis mechanisms have been deciphered for decades, whether cell respiration is controlled by [ATP]/[ADP] or [ATP]/[ADP][Pi] ratios (1, 2), by the adenylate energy charge ([ATP + 0.5 ADP]/[ATP + ADP + AMP]) (3, 4), and/or by the concentration of ATP or ADP in the cytosol (5, 6) remains a matter of debate. To our knowledge, the determining factor for controlling cell respiration in response to the energy demand has not yet been unambiguously characterized.

MgATP is the substrate of numerous phosphorylating enzymes and the principal energy source of the cell. Indeed, any increase in metabolic activity increases the rate of MgATP use and, consequently, the rate of ADP and magnesium release, and vice versa. In normoxia, the MgATP concentration should be essentially balanced by the ADP phosphorylation catalyzed by mitochondrial ATP synthase, thereby adjusting oxidative phosphorylation to cell ATP needs. The ADP/ATP carrier (AAC) of the inner mitochondrial membrane, which exchanges free nucleotides, and adenylate kinase (EC 2.7.4.3), which interconverts MgADP and free ADP with MgATP and free AMP in the presence of Mg^{2+} (7), participate in this regulation (reviewed in ref. 8). Clearly, to better understand the interplay of free and Mg-complexed ADP and ATP in the regulation of cell respiration it is necessary to know their concentrations, as well as the concentration of Mg^{2+} in the cytosol and mitochondrial matrix.

Nucleotides can be measured using ^{31}P-NMR spectroscopy both in vitro, from cell extracts, and in vivo, in perfused material. After 1 h of data accumulation time, detection thresholds are approximately 20 nmol in vitro and 50 nmol in vivo (9). Various techniques for measuring intracellular [Mg^{2+}] and free/Mg-complexed nucleotides have been proposed (10–12), but none allows measurement in different intracellular compartments. In vivo ^{31}P-NMR spectroscopy offers this possibility, because the chemical shift (δ) of the γ- and β-phosphorus resonances of ATP and the β-phosphorus resonance of ADP depend on pH and [Mg^{2+}] (13). We adapted this noninvasive technique to the simultaneous in vivo measurement of cytosolic and mitochondrial Mg^{2+} and free/Mg-complexed nucleotides concentrations in culture cells.

We used homogenous cells cultivated on liquid nutrient media (NM) so as to narrow resonance peaks on in vivo NMR spectra, thus improving the signal-to-noise ratios and the accuracy of chemical shift measurements and limiting peak overlaps. In addition, the heterotrophic sycamore (*Acer pseudoplatanus* L.) cells of cambial origin used in this study contain no large chloroplasts, but only small plastids (14, 15) with low amounts of nucleotides (16), thus permitting more precise measurement of the cytosolic and mitochondrial nucleotide pools.

Significance

The respiration of heterotrophic cells, where most of the ATP demand is met by mitochondrial oxidative phosphorylation, is generally thought to be regulated either by the ATP/ADP ratio and/or energy charge or by nucleotide concentration. The way in which ADP and ATP may directly mediate respiration remains unclear, however. Furthermore, because only free nucleotides are exchanged by the mitochondrial ADP/ATP carrier, whereas MgADP is the substrate of ATP-synthase, Mg^{2+} compartmentation must be known. For this purpose, we performed simultaneous measurements of free and Mg-complexed nucleotides and Mg^{2+} in the cytosol and mitochondrial matrix using NMR-based techniques. Physiological alterations induced by Mg starvation helped unravel the key role of cytosolic and mitochondrial Mg^{2+} and free ADP in the regulation of cell respiration.

Author contributions: R.D. and R.B. designed research; E.G. and R.B. performed research; E.G., F.R., R.D., and R.B. analyzed data; and F.R. and R.B. wrote the paper.

The authors declare no conflict of interest.

This article is a PNAS Direct Submission.

[1]To whom correspondence should be addressed. Email: rbligny@cea.fr.

This article contains supporting information online at www.pnas.org/lookup/suppl/doi:10.1073/pnas.1406251111/-/DCSupplemental.

To modify nucleotide concentrations without using inhibitors that may interfere with mitochondrial functioning, we varied the cell culture media: standard, adenine-supplied, Pi-starved, and Mg-starved. In this paper, we refer to cytoplasm as the cell compartment exterior to the vacuole and cytosol as the cell compartment exterior to the vacuole and the organelles bounded by a double membrane (mitochondria and plastids).

The aim of the present study was to determine the role of ADP, ATP, and Mg^{2+} concentrations in the in vivo control of mitochondrial respiration. We show that the balance between cytosolic and mitochondrial free ADP, depending on the concentration of Mg^{2+} in the cytosol and matrix, mediates this regulation.

Results

In Vivo Measurement of Nucleotide Pools in Sycamore Cells Cultivated in Standard, Adenine-Supplied, and Pi-Free NM. An in vivo ^{31}P-NMR spectrum of oxygenated sycamore cells (10 g) perfused with a standard NM containing 50 μM phosphate at pH 6.0 shows two peaks of inorganic phosphate (Pi) present in the cytoplasm (cyt-Pi) at pH 7.6 and in the vacuole (vac-Pi) at pH 5.7 (Fig. 1*A*). We previously showed that the cyt-Pi peak itself contains two partially overlapping Pi peaks corresponding to Pi pools located in mitochondria and plastids at pH 7.55–7.65 (the main peak) and in the cytosol at pH 7.40 (9). Among sugar phosphates, glucose 6-P and fructose 6-P provide the major well-identified peaks. Nucleotide triphosphates (principally ATP) were identified from three peaks corresponding to γ-, α-, and β-phosphorus at −5.45, −10.6, and −19.2 ppm, respectively. The area under the γ-ATP peak represented here corresponds to approximately 700 nmol, indicating that the cell ATP concentration was ~70 nmol g^{-1} cell wet weight. The main nucleotide sugar, uridine-5′-diphosphate-α-D-glucose (UDP-glc), was identified from the two pairs of doublets centered at −11.1 and −12.8 ppm, corresponding to the β- and α-phosphorus of the molecule. No peak corresponding to ADP was unequivocally identified in the 1-h spectra.

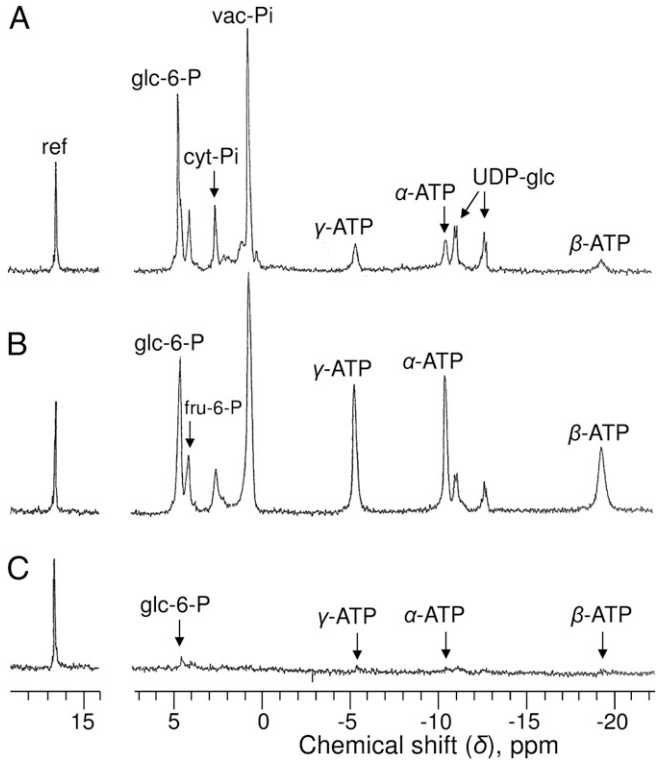

Fig. 1. In vivo proton-decoupled ^{31}P-NMR spectra of sycamore cells. (*A*) Cells harvested in NM at 5 d after subculture and perfused in a 25-mm NMR tube with a well-oxygenated diluted NM. (*B*) Cells preincubated in adenine-supplied NM for 12 h and perfused in the presence of 1 mM adenine. (*C*) Cells preincubated in Pi-free NM for 5 d and perfused with Pi-free NM. Acquisition time, 1 h (6,000 scans). Peak assignments: ref, reference (methylenediphosphonate) used to measure chemical shifts and for quantification; glc-6-P, glucose 6-phosphate; fru-6-P, fructose 6-phosphate.

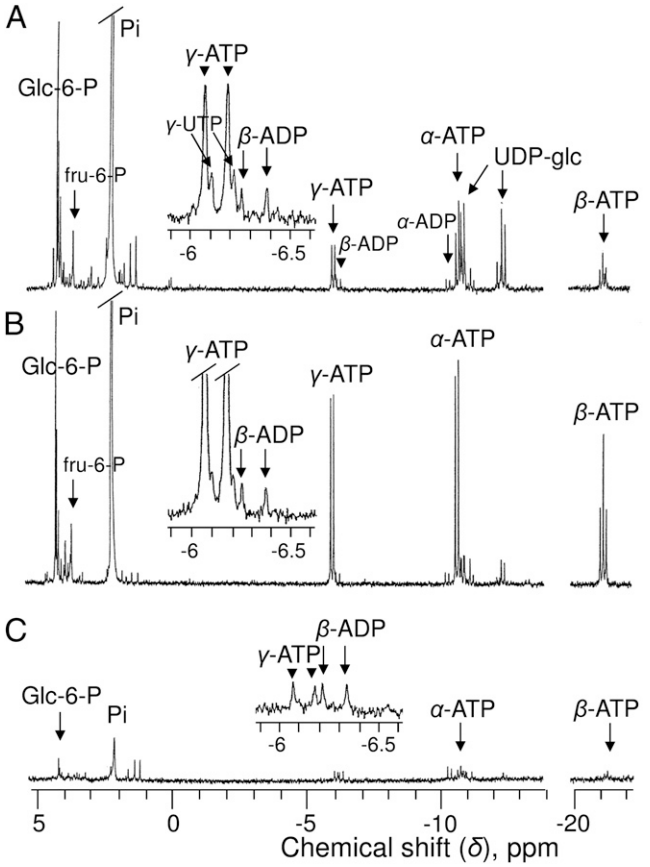

Fig. 2. Proton-decoupled ^{31}P-NMR spectra of PCA extracts of sycamore cells. Cells in *A*–*C* were cultivated under the same conditions as in Fig. 1 *A*–*C*: rapidly rinsed with water, strained, and frozen in liquid nitrogen before PCA extraction. (*Insets*) Enlarged portions of spectra centered on γ-ATP at −6.2 ppm. Note that the chemical shifts of β- and γ-ATP are different from their in vivo values (upfield shift) because divalent cations, including Mg^{2+}, are chelated during PCA extract preparation. Peak assignments are as in Fig. 1. UTP, uridine triphosphate. Acquisition time, 1 h (1,024 scans).

In cells preincubated for 12 h in NM containing 1 mM adenine, [ATP] increased fivefold (Fig. 1*B*), reaching 340 nmol g^{-1} cell wet weight. Sugar phosphate and Pi pools were not significantly modified, and ADP remained below the in vivo ^{31}P-NMR detection threshold.

In contrast, after a 5-d incubation in Pi-free NM, all soluble P-compounds decreased dramatically (Fig. 1*C*), reaching (or being below) the detection threshold. To measure P-compound concentrations in this case, as well as to measure ADP concentrations in all incubation conditions, it was necessary to improve the signal-to-noise ratio. One way to do this is to perform measurements from cell extracts.

Measurement of Nucleotides from Cell Extracts and ADP Homeostasis. The in vitro ^{31}P-NMR analysis of series of cell extract (Fig. 2*A*) permitted more precise measurement of [ATP] (68 ± 7 nmol g^{-1} cell wet weight in standard cells). Other nucleotide triphosphates, such as uridine triphosphate, were poorly abundant regardless of the culture conditions. As expected, ADP was unambiguously

identified from its doublets of α- and β-peaks centered at −6.35 and −10.4 ppm, respectively. [ADP] was 11 ± 2 nmol g^{-1} cell wet weight. The peak of AMP (at 3.7 ppm) was too small for quantification. Other spectra (Fig. 2 *B* and *C*) confirm that ATP varied significantly in relation to NM composition, increasing fivefold in adenine-supplied cells or decreasing sixfold in Pi-starved cells. In this latter case, sugar phosphate decreased by more than 90%. However, the most striking observation is that the concentration of ADP remained almost unchanged regardless of the cell incubation NM, adenine-supplied, or Pi-deprived.

These results are summarized in the histogram of Fig. 3 and extended to cultures maintained at low temperature (5 °C) and after a 12-h incubation in the presence of choline and glycerol, which are readily phosphorylated (17, 18). Here again, [ADP] did not differ significantly from that of standard cells, whereas [ATP] increased at low temperature and decreased in the presence of choline and glycerol. Significant modifications of [ADP] were observed only after incubating cells in Mg-free NM (developed at the end of *Results* section), and under hypoxic conditions.

Concentrations of ATP and ADP in Different Cell Compartments. Assuming that the cytoplasm occupies 15% of the cell volume in exponentially growing sycamore cells (14), the concentrations of ATP and ADP in the cytoplasm of standard cells were 450 ± 40 μM and 73 ± 13 μM, respectively. These concentrations are still global, however, and do not take the cytoplasmic microcompartmentation into account. For example, the possibility that the cytosol contains only a small ADP pool that may vary according to culture conditions and constitute a metabolic signal, whereas more important ADP pools present in organelles remain stable, cannot be excluded. The cytosolic ADP can be calculated by subtracting the mitochondrial and plastidial ADP pools from the total cell ADP. Mitochondrial ADP was measured in perchloric acid (PCA) extracts of purified sycamore cell mitochondria, using ^{31}P-NMR (19). Plastidial ADP was measured similarly in purified amyloplasts (20).

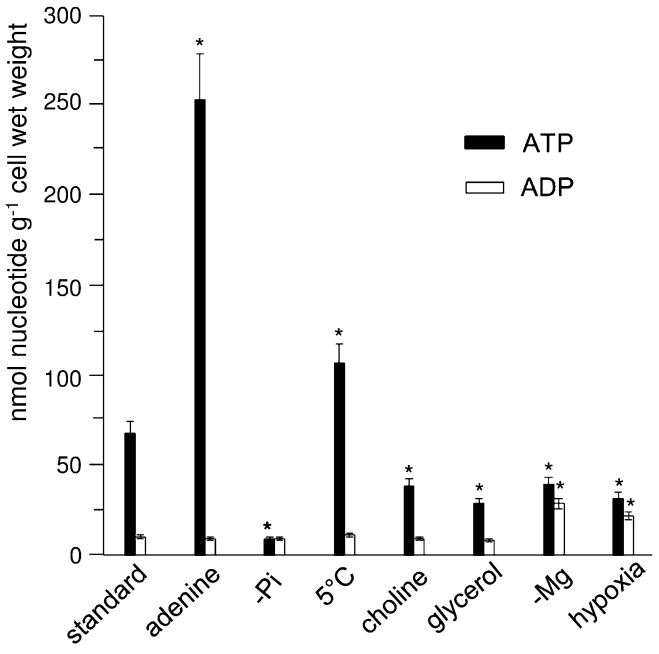

Fig. 3. Concentrations of ATP and ADP in sycamore cells incubated in different media. Measurements were performed from proton-decoupled ^{31}P-NMR spectra of PCA extracts. Specific preincubation times: 1 mM adenine, 12 h; –Pi, 5 d; 5 °C, 20 d; 0.1 mM choline, 12 h; 50 mM glycerol, 12 h; –Mg, 2 wk; anoxia, 20 min. Error bars indicate mean ± SEM; $n = 5$. *Values that differ significantly ($P \leq 0.05$) from the corresponding values of the reference sample on the Student *t* test.

Table 1. Quantification of ATP and ADP in different subcellular compartments of sycamore cells

	Cytoplasm	Mitochondria	Plastids	Cytosol
ATP	68 ± 7	9.0 ± 1.0	3.0 ± 1	56 ± 6
ADP	11 ± 2	4.0 ± 1	3.5 ± 1	3.5 ± 1

Cells were cultivated in standard NM as indicated in Fig. 1. Nucleotide quantification was performed from ^{31}P-NMR analysis of PCA extracts of cell and isolated mitochondria and plastids, by subtracting mitochondrial and plastidial values from cytoplasmic ones for cytosolic measurement. The cell proportions of cytoplasm, matrix, and stroma were taken as 15.3%, 1.7%, and 1.6%, respectively (14). Values correspond to nmol g^{-1} cell wet weight and are reported as mean ± SD ($n = 5$).

From the quantity of nucleotides measured in these different compartments (Table 1), we calculate that 32% of sycamore cell ADP is located in the cytosol and 68% is located in organelles (mitochondria, 36%; plastids, 32%), whereas 82% of ATP is present in the cytosol and 18% in organelles (mitochondria, 13%; plastids, 4.4%).

These results do not discriminate between free and Mg-complexed nucleotides, however. Because only free nucleotides are transported by the AAC, the knowledge of their concentration and that of Mg^{2+} in the cytosol and matrix was required to better understand the role played by the mitochondrial nucleotide transporter in the regulation of cell respiration.

In Vivo Measurement of Free and Mg-Complexed ATP and Mg^{2+} in the Cytosol. Because the cytosol contains 82% of cell ATP (Table 1), the ATP peaks detected in vivo (Figs. 1 and 4*A*) correspond mainly to the ATP pool present in this compartment (at pH 7.4). Consequently, the chemical shift of the γ-phosphorus of ATP ($\delta_{\gamma\text{-ATP}}$) (−5.45 ppm) must be related to the calibration curve established at pH 7.4 (Fig. S1). It gives a free/Mg-complexed ATP ratio of 0.135. The $\delta_{\gamma\text{-ATP}}$ (−5.45 ppm) approaches the upper limit of γ-ATP chemical shift (−5.30 ppm; Fig. S1), but ATP was not fully saturated with Mg^{2+} as shown at the end of result section. The precision of the measurements based on the $\delta_{\gamma\text{-ATP}}$ was approximately 10%. The cytosolic [free-ATP] and [MgATP] measured from the sum (Table 1) and the ratio of their free and Mg-complexed forms are 54 ± 6 μM and 400 ± 50 μM, respectively (Table 2).

The concentration of Mg^{2+} in the cytosol can be calculated from the MgATP dissociation constant K_d^{MgATP} and the [free-ATP]/[MgATP] ratio measured at pH 7.4, as described in *Materials and Methods*. Given a K_d^{MgATP} determined as 35 ± 3 μM, the cytosolic [Mg^{2+}] was calculated to be 250 ± 30 μM. The in vitro simulation spectrum obtained with this Mg^{2+} concentration (Fig. 4*B*) fits to the in vivo cell spectrum (Fig. 4*A*). This concentration is in the 200–400 μM range reported in the cytosol of erythrocytes (22) and different plant cells (12). In addition, the stability of the chemical shift of γ-ATP regardless of the cell incubation conditions, except under anoxia and Mg starvation, indicates that the [free-ATP]/[MgATP] ratio is constant and, consequently, the cytosolic [Mg^{2+}]. In particular, the $\delta_{\gamma\text{-ATP}}$ was the same in standard cells, in adenine-supplied cells massively accumulating ATP, and in Pi-deficient cells containing a low ATP concentration (Fig. 1), indicating that the cytosolic [Mg^{2+}] is tightly buffered by Mg^{2+} exchanges with intracellular stores.

In Vivo Measurement of Free and Mg-Complexed ADP in the Cytosol. When cells are perfused with a hypoxic NM triggering the drop in ATP, the accumulation of ADP (~40 nmol g^{-1} cell wet weight), and the decrease in cytosolic pH to 6.8 (23), a clear peak corresponding to the β-phosphorus of ADP ($\delta_{\beta\text{-ADP}}$) appears at −6.6 ppm within minutes, together with a shoulder on the left side of

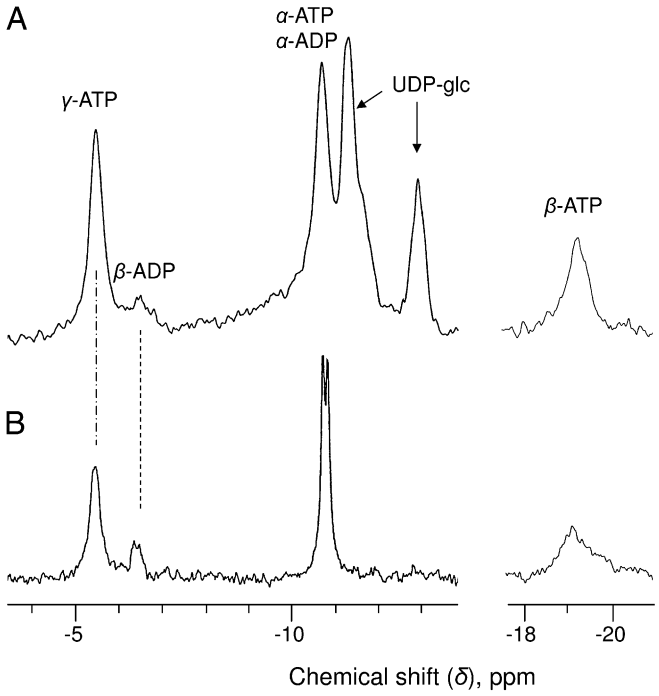

Fig. 4. Enlarged portions of in vivo proton-decoupled ^{31}P-NMR spectra of sycamore cells (*A*) and a solution of ATP + ADP (*B*). (*A*) Cells harvested at 5 d after subculture in standard medium and perfused as described in Fig. 1. Acquisition time, 16 h (96,000 scans). The 16-h spectrum is the sum of four successive 4-h blocks showing no change across the 16-h time course of the experiment. This fragmentation of the data accumulation time allowed us to check the stability of the spectrum. (*B*) Solution of 0.6 mM ATP + 0.15 mM ADP containing 0.8 mM $MgSO_4$, 150 mM KNO_3, and 20 mM Hepes buffer (pH 7.4) analyzed in a 10-mm NMR tube. Acquisition time, 15 min (1,500 scans).

α-ATP corresponding to the α-phosphorus of ADP (Fig. S2 *A* and *B*). In contrast, no β-ADP was detected in spectra of oxygenated cells after 1 h of data accumulation (Fig. 1). Of course, normoxic cells contain only 11 nmol of ADP g^{-1} (Table 1), but this should be detected, given that this value is twice the in vivo nucleotide detection threshold (50 nmol). Because this was not the case, we hypothesized that the β-peak of the ADP pool located in organelles was distinct from the cytosolic one (downfield shift observed at high [Mg^{2+}]) and overlapped by the γ-peak of ATP. In that case, the cytosolic ADP, which represents one-third of total cell ADP (Table 1), should be below the detection threshold.

To improve the signal-to-noise ratio, data were accumulated over 16-h as the sum of four successive identical blocks of 4 h. In that case, a small peak was observed between −6.30 and −6.40 ppm, quite distinct from that of γ-ATP (−5.45 ppm), which was attributed to β-ADP (Fig. 4*A*). The area under this peak indicates that the size of the cytosolic ADP pool was 3.6 ± 0.6 nmol g^{-1} cell wet weight, close to the value calculated in Table 1. Similar values were measured from adenine-supplied or Pi-deprived cell spectra (Fig. S3).

From the $\delta_{\beta\text{-ADP}}$ (−6.35 ppm) and the calibration curve at pH 7.4, we calculate that approximately 71% of the cytosolic ADP is free and the other 29% is complexed to Mg^{2+}. The corresponding [free ADP] and [MgADP] values are 20 ± 2 μM and 9 ± 1 μM, respectively (Table 2). The cytosolic concentration of Mg^{2+} calculated from the K_d^{MgADP} is 670 ± 50 μM, and the [free-ADP]/[MgADP] ratio is close to 250 μM, confirming the value measured from the $\delta_{\gamma\text{-ATP}}$. Here again, the in vitro simulation (Fig. 4*B*) fit to the in vivo spectrum. Finally, in vivo 16-h spectra of adenine-supplied cells and Pi-deprived cells (Fig. S3) show a constant $\delta_{\beta\text{-ADP}}$, increasing confidence in the conclusion that cytosolic [Mg^{2+}] is stable.

Measurement of Free and Mg-Complexed ATP and ADP and of Mg^{2+} in Mitochondria. Because of their low cell amount and overlaps with cytosolic γ-ATP, mitochondrial nucleotides could not be directly measured in cell spectra. For this reason, we isolated physiologically active intact mitochondria from large amounts of packed cells, as described in *Materials and Methods*. The ^{31}P-NMR spectra of 2 mL of the thick slurry of mitochondria (0.2 g protein/mL) analyzed in suspension in their Pi- and Mg-free purification medium allowed us to identify the ATP and ADP pools from their γ- and β-phosphorus, respectively (Fig. 5*A*). In contrast, the chemical shift of the abundant matrix Pi (19) was 1.95 ppm, indicating that the pH of the matrix was 7.0. The $\delta_{\gamma\text{-ATP}}$ at −5.32 ppm referred to the calibration curve at pH 7.0 (Fig. S1) indicates that >98% of this nucleotide was complexed to Mg^{2+}, whereas <2% was in the free form. The $\delta_{\beta\text{-ADP}}$ value between −6.15 and −6.25 ppm indicates

Table 2. Free- and Mg-complexed ATP and ADP and Mg^{2+} concentrations in the cytosol and mitochondria of sycamore cells

	Standard conditions		Mg-free conditions	
	Cytosol	Mitochondria	Cytosol	Mitochondria
Free ATP, μM	54 ± 6	10 ± 2	110 ± 15	95 ± 20
Mg-complexed ATP, μM	400 ± 50	520 ± 60	260 ± 30	240 ± 40
Free ADP, μM	20 ± 2	45 ± 8	100 ± 15	180 ± 30
Mg-complexed ADP, μM	9 ± 1	180 ± 30	6 ± 2	40 ± 10
Mg^{2+}, μM	250 ± 30	2,400 ± 400	45 ± 5	70 ± 15

Cells were cultivated and harvested as indicated in Fig. 1, under standard and Mg-free conditions. Free and Mg-complexed nucleotide quantifications in the cytosol and mitochondria were performed from cell extracts and from in vivo ^{31}P-NMR analyses as described in the text. Concentrations were calculated assuming that the cytosol and the matrix occupy 12% and 1.7% of the volume of cells, respectively (14). Values are mean ± SD (n = 5).

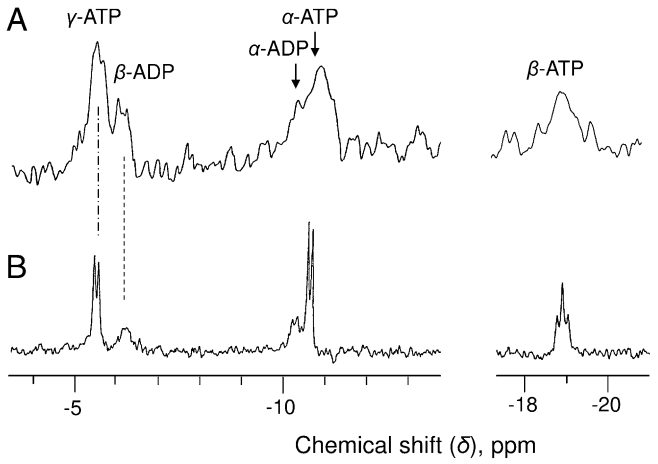

Fig. 5. Enlarged portions of proton-decoupled ^{31}P-NMR spectra of sycamore cell mitochondria (*A*) and a solution of ATP + ADP (*B*). (*A*) Mitochondria purified from 2 kg of cells harvested after 5-d subculture in standard medium. Here 2 mL of mitochondrial suspension (0.2 g protein/mL) was placed in a 10-mm NMR tube in purification medium containing 0.3 M mannitol, 20 mM Hepes buffer (pH 7.0), and 0.1% BSA. Acquisition time, 2 h (12,000 scans). This spectrum is the sum of the first two 1-h spectra, which were identical. (*B*) Solution of 0.6 mM ATP + 0.15 mM ADP containing 2.5 mM $MgSO_4$, 150 mM KNO_3, 0.3 M mannitol, and 20 mM Hepes buffer (pH 7.0) analyzed in a 10-mm NMR tube. Acquisition time, 15 min (1,500 scans).

that nearly 80% of matrix ADP was complexed to Mg^{2+}, with the remaining 20% in the free form. Because the $\delta_{\gamma\text{-ATP}}$ was too close to the endpoint of the titration curve, the mitochondrial [Mg^{2+}] was calculated from the $\delta_{\beta\text{-ADP}}$ giving the [free ADP]/[MgADP] ratio, and the K_d^{MgADP} (670 ± 50 μM). Its value (2.4 ± 0.3 mM) was confirmed by the comparison with the simulation assay (Fig. 5*B*). This concentration is also relatively close to the 4 mM reported in potato tuber mitochondria from succinate- and α-ketoglutarate-Mg^{2+}–dependent respiration measurements (21).

Of course, the possibility that some amount of Mg^{2+} is lost during mitochondrial preparation cannot be excluded. In that case, the [Mg^{2+}] gradient between the cytosol and matrix would be higher, thus favoring the import of ADP into mitochondria, as discussed below. On the basis of mitochondrial proteins, [Mg^{2+}] (6.5 ± 0.8 nmol/mg) represents approximately 36% of the total mitochondrial magnesium measured from inductively coupled mass spectrometry (ICP-MS) analysis (18 ± 2 nmol/mg). Free and complexed mitochondrial nucleotide concentrations in the cytosol were calculated as described above (Table 2).

The finding that cells incubated in various NM contain low and stable [ADP] but variable [ATP] suggests that ADP, unlike ATP, exerts a tight control on respiration. This control can occur at the level of either AAC or ATP synthase. Concerning the first possibility, given that only free nucleotides are exchanged across the inner mitochondrial membrane, it may be proposed that the low cytosolic [Mg^{2+}] leading to a high [free ADP]/[MgADP] ratio in the cytosol, and the reciprocal in the matrix, facilitates ADP import into the mitochondria. To analyze this hypothesis, we cultivated cells in Mg-free NM so as to modify the free to Mg-complexed nucleotide balance in the cytosol and matrix, and measured cell respiration and growth simultaneously.

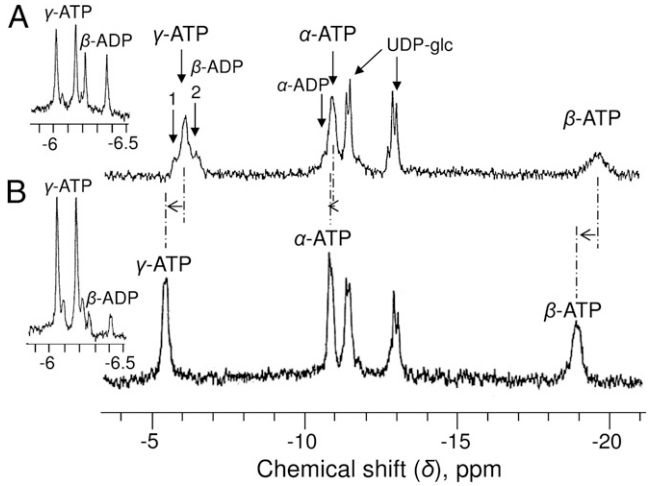

Fig. 6. Enlarged portions of in vivo proton-decoupled ^{31}P-NMR spectra of sycamore cells. (*A*) Cells harvested after a 2-wk preincubation in Mg^{2+}-free NM and perfused with Mg^{2+}-free NM. Acquisition time, 4 h (24,000 scans). The spectrum is the sum of four successive comparable 1-h spectra. Peak 1 was attributed to the γ-signal of mitochondrial ATP, and the broad peak 2 was attributed to the β-signal of ADP pools present in mitochondria and cytosol. (*B*) Spectrum accumulated 1 h after the addition of 1 mM $MgSO_4$ to NM. Perfusion conditions are as in Fig. 1 with standard NM. Acquisition time, 1 h (6,000 scans). Horizontal arrows indicate the downfield shift (toward the left of the spectra) of the different ATP resonance peaks after the addition of $MgSO_4$ to NM. (*Insets*) Centered on γ-ATP at −6.2 ppm, portions of PCA extract spectra prepared from cells incubated outside the magnet under the same conditions. Acquisition time, 1 h (1,024 scans).

Effect of Mg Starvation on Free and Mg-Complexed Nucleotides in Cytosol and Matrix. Sycamore cells were first grown in Mg-free NM over 2 wk to exhaust cell magnesium stores, particularly abundant in the vacuole (24). Indeed, during the first 10 d of Mg starvation, the $\delta_{\gamma\text{-ATP}}$ value remained unchanged, confirming that the cytosolic [Mg^{2+}] was buffered by the release of Mg^{2+} from intracellular stores. Subsequently, the ATP peaks began to shift upfield (toward the right of spectra) (Fig. 6*A*), reflecting a decrease in cytosolic [Mg^{2+}]. After 2 wk, the initial magnesium content of cells measured by ICP-MS on PCA extracts had decreased from 8.5 ± 2 to 1.5 ± 0.3 μmol g^{-1} cell wet weight. At that stage, the cell growth stopped, and cell respiration began to decrease (Table 3). In addition, cells became unable to rapidly phosphorylate added adenine, choline, or glycerol (Table S1). Nevertheless, the cytoplasmic pH measured from the $\delta_{cyt\text{-}Pi}$ remained stable, indicating that the proton pump ATPases were still working. We assume below that the cytosolic and mitochondrial pHs were not affected. Simultaneously, the cell ATP decreased from 68 ± 7 to 41 ± 5 nmol g^{-1} cell wet weight, whereas ADP symmetrically increased from 11 ± 2 to 35 ± 4 nmol g^{-1} cell wet weight (calculated from PCA extracts; Fig. 6*A*, *Inset*). The in vivo spectra of 2-wk Mg-free cells confirm the decrease in ATP (Fig. 6*A*) and, based on the $\delta_{\gamma\text{-ATP}}$ (−5.90 ppm), indicates that 65% of the cytosolic ATP was still complexed to Mg^{2+}. The cytosolic [Mg^{2+}] calculated from this value was 45 ± 10 μM.

Of particular interest were the peak 1 at −5.60 ppm on the left side of γ-ATP and the broad signal between −6.40 and −6.70 ppm on the right side (Fig. 6*A*). Based on its δ value, peak 1 should correspond to a pool of ATP located in a cell compartment containing a higher concentration of Mg^{2+} than the cytosol and, consequently, the mitochondria. Based on the calibration curve at pH 7.6, the in vivo pH of the matrix, this δ value indicates that at least 30% of mitochondrial ATP was free and that [Mg^{2+}] decreased to <100 μM. The broad signal on the right side of γ-ATP very likely corresponds to the important ADP pool identified on PCA extraction (Fig. 6*A*, *Inset*). Given the cytosolic and mitochondrial [Mg^{2+}] calculated above, we propose that this results from the juxtaposition of the β peaks of mitochondrial ADP (at ∼ −6.30 ppm) and cytosolic ADP (at ∼ −6.60 ppm), which are not resolved. Accordingly, in these Mg-deficient cells, >70% of mitochondrial ADP and 90% of cytosolic ADP were free. The concentrations of free and Mg^{2+}-complexed nucleotides in the cytosol and mitochondria of Mg-deficient cells (Table 2) were calculated from the PCA extract data, giving the total amount of ADP and an estimate of the cytosolic β-ADP peak area.

Table 3. Coupled and uncoupled respiration rates of sycamore cells

Respiration	Standard	+ Adenine	Pi-free	Mg-free	+ Mg (1 h)
Coupled	0.35 ± 0.02	0.37 ± 0.02	0.30 ± 0.02*	0.20 ± 0.03*	0.32 ± 0.02
Uncoupled	0.55 ± 0.04	0.53 ± 0.04	0.51 ± 0.05	0.46 ± 0.05	0.48 ± 0.04

Cells were incubated in standard, 1 mM adenine-supplied (12 h), Pi-free (5 d), Mg-free (14 d), and 1 h after the addition of Mg to Mg-free NM. For respiration measurements, 50 mg of cells were placed in a 1-mL O_2 electrode chamber. The temperature of incubation was 20 °C. Cell respiration rates are expressed as μmol O_2 consumed min^{-1} g^{-1} cell wet weight. The uncoupled cell respiration was measured in presence of 2 μM FCCP. Values are mean ± SD ($n = 5$). *Values that differ significantly ($P \leq 0.05$) from the corresponding values of the standard cells in the Student *t* test.

At 1 hr after the addition of 1 mM Mg^{2+} to NM, the different nucleotide peaks moved downfield, indicating that Mg^{2+} was quickly incorporated into the cytosol and mitochondria. Interestingly, the $\delta_{\gamma\text{-ATP}}$ first shifted to −5.35 ppm (Fig. 6*B* and Fig. S4*A*) before recovering, after 2 h, to the −5.45 ppm value measured in standard cells (Fig. S4*B*). The constant δ_{cytPi} (2.40 ppm) and cytostolic pH indicate that the cytosolic [Mg^{2+}] transiently exceeded 250 μM and that ATP was not fully saturated with Mg^{2+} under normal conditions. The recovery also confirms that on in vivo spectra, the β peak of mitochondrial ADP is overlapped by the γ peak of cytosolic ATP. The magnesium deficiency separated these peaks. Simultaneously, the cytosolic β-ADP peak became undetectable, whereas the γ-ATP peak area recovered to a standard value. PCA extract analysis (Fig. 6*B*, *Inset*) confirms that ADP accumulated in Mg-starved cells was promptly phosphorylated by ATP synthase.

Cell Respiration in Standard, Adenine-Supplied, Pi-Free, and Mg-Free NM. The O_2-uptake rates of sycamore cells harvested during their exponential phase of growth and incubated for 12 h at 20 °C in standard and adenine-supplied NM were identical (Table 3). A small difference attributable to the arrest of cell growth (9) was observed in cells incubated for 5 d in a Pi-free NM. This difference was surprisingly small compared with the dramatic decrease in ATP. In contrast, the O_2-uptake rate of cells incubated for 2 wk in Mg-free NM diminished by nearly 43%, and cell survival became compromised after this period. Indeed, the maintenance of Mg^{2+} homeostasis is essential for the viability of plant cells (reviewed in ref. 25). No significant difference in the uncoupled O_2-uptake rates was observed in the various situations when 2 μM cyanide *p*-trifluoromethoxyphenylhydrazone (FCCP), an uncoupling agent, was added to cell suspensions. Even after 2 wk of Mg starvation, the uncoupled cell respiration rate (0.5 μmol O_2 consumed min^{-1} g^{-1} cell wet weight) did not differ significantly from that of standard cells (Table 3), indicating that the concentration of Mg^{2+} in matrix was still sufficient to permit the oxidation of respiratory substrates at maximum rate. At 1 hr after the addition of Mg^{2+} to NM, the respiration of Mg-deficient cells recovered to a standard value, together with ATP and ADP concentrations and chemical shifts, as described above (Fig. 6*B*).

Discussion

In this report, we show that the concentration of ADP in suspension-cultured sycamore cells remains remarkably constant and low (11 ± 2 nmol g^{-1} cell wet weight) irrespective of cell incubation conditions, except for magnesium deficiency and anoxia. Of course, we have previously used ^{31}P-NMR to detect low [ADP] in different plant materials, including lichens (26), maize root tips (27), and sunflower cotyledons (28), but the present work is the first study in which [ADP] is seen to be so stable. In marked contrast, [ATP] may vary very widely. For example, incubation in the presence of adenine results in a huge increase in [ATP], with no changes in cell respiration and growth. In contrast, in the case of Pi starvation or increased cell phosphorylation activity in the presence of choline or glycerol, [ATP] decreases, unlike [ADP]. This suggests that [ADP] is tightly controlled, and that any modification in ADP release immediately triggers the required adjustments to oxidative phosphorylation in mitochondria. This homeostasis of ADP questions the significance of [ATP]/[ADP] or [ATP]/[ADP][Pi] ratios and adenylate energy charge as regulators of cell respiration. The microcompartmentation of cell adenylates should be considered (12), as should the chemical form (free or Mg-complexed) in which each nucleotide is present. The way in which these different parameters may interact is schematized in Fig. 7.

Mg^{2+} Homeostasis and Dissymmetry Between Cytosol and Mitochondrial Matrix. The γ-ATP and β-ADP chemical shifts were found to be stable under different physiological conditions, including adenine supply and Pi deficiency. They decreased only in the case of magnesium deficiency and increased transiently above standard values during the recovery after the addition of Mg^{2+} to NM. The remarkable stability of $\delta_{\gamma\text{-ATP}}$ and $\delta_{\beta\text{-ADP}}$ suggests that the cytosolic [Mg^{2+}] is closely regulated and raises the possibility of a compensating release of Mg^{2+} from the vacuole, in which the major part of cellular magnesium is sequestered (25). The $\delta_{\gamma\text{-ATP}}$ and $\delta_{\beta\text{-ADP}}$ values (−5.45 and −6.35 ppm) measured in standard cells indicate a low cytosolic [Mg^{2+}] value (close to 250 μM). In contrast, [Mg^{2+}] is tenfold higher (2.4 mM) in purified mitochondria. This high [Mg^{2+}] restricts the [free ATP] in mitochondria to <20% of its value in the cytosol, which constitutes a countergradient for its export. However, in adenine-supplied cells containing fivefold more free ATP in their cytosol, cell respiration and growth were not modified despite a still higher free ATP countergradient. This finding suggests that mitochondrial low [free ATP] does not limit ADP/ATP exchange in that case, even more so in standard cells.

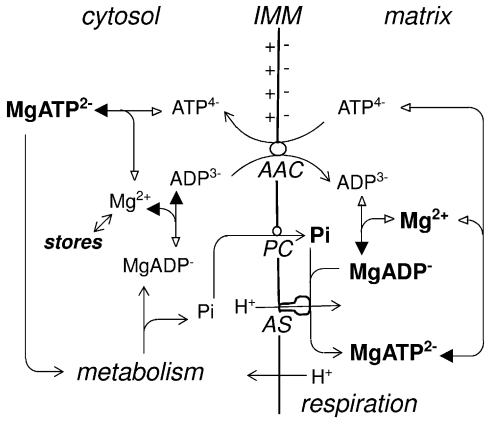

Fig. 7. Recycling of free and Mg-complexed nucleotides and Mg^{2+} in the cytosol and mitochondrial matrix in response to cell demand for energy. AAC, ADP/ATP carrier; AS, ATP-synthase; PC, phosphate-carrier; IMM, inner mitochondrial membrane. Note that the scheme is simplified and does not show adenylate kinase or describe the H^+ gradient-generating process. Bold characters indicate the most abundant compounds, and solid arrowheads indicate the privileged direction of free vs. Mg^{2+} nucleotide equilibriums.

In contrast, the dissymmetry between cytosolic and mitochondrial [Mg^{2+}] maximizes cytosolic [free ADP] and minimizes mitochondrial [free ADP], which favors ADP import. Nevertheless, the mitochondrial [Mg^{2+}] level is still not sufficiently high to render [free ADP] lower in mitochondria than in cytosol (Table 2). Thus, the free nucleotide repartition between cytosol and mitochondria should prevent ADP import and ATP export according to a 1:1 exchange. In fact, the electrogenic ADP^{3-}/ATP^{4-} exchange against concentration gradients occurs when mitochondria are in the energized state, because the ADP influx/ATP efflux ratio is then multiplied by a factor of close to 20 (29). In particular, high-resolution mapping of the AAC has recently shown that ADP^{3-} is driven through an electrostatic funnel in energized mitochondria (30).

Cytosolic Free ADP Homeostasis. Cytosolic ADP represents a minor but stable fraction of the total cell ADP (3.5 ± 0.5 vs. 11 ± 2 nmol g^{-1} cell wet weight). As a consequence of Mg^{2+} homeostasis, the cytosolic [free ADP] is also stable (20 ± 2 μM). This value is close to the reported K_m of the adenylate carrier for ADP of between 15 μM (31) and 40 μM (32). Consequently, any modification of cytosolic [free ADP] would affect the rate of ADP import within the mitochondria. In particular, small NMR-undetectable changes of cytosolic [free ADP] should impact the ADP/ATP exchange rate between the cytosol and mitochondria and, consequently,

respiration. This kind of control has been reported in relation to the steady-state oxidative phosphorylation in rat gastrocnemius (33). Interestingly, a comparable situation regarding Pi compartmentation was observed in sycamore and *Arabidopsis* cells, where low cytosolic [Pi] plays an important role in cell metabolism regulation (9).

Origin of Respiration and ATP Decrease in Mg^{2+}-Starved Cells. After 2 wk of Mg starvation, cell growth stopped and respiration decreased, indicating that the activity of key MgATP-requiring enzymes was affected, as was observed for choline and glycerol kinases. Indeed, most ATPases use MgATP, and in Mg-starved cells, cytosolic MgATP decreased by nearly 35%. In contrast, glycolysis still delivered sufficient respiratory substrates to fuel uncoupled respiration at a maximal rate, and proton pumps still functioned, because intracellular pH was not affected. Why did the respiration of Mg-starved cells decrease by a factor of nearly two under these conditions, but not in other situations of growth arrest, such as that provoked by Pi deficiency? A possible explanation could be that ATP synthase became rate-limiting for respiration owing to the decrease in the matrix of [MgADP] from 180 to 40 μM. Indeed, the apparent K_m of ATP synthase for MgADP calculated in isolated mitochondria from respiration curves (19) is close to 30 μM. The accumulation of ADP at the expense of ATP tends to confirm this hypothesis. In addition, because free ADP/free ATP exchange is inhibited by the opposite adenylate with K_i comparable to K_m (34), ATP export from mitochondria would be hampered by excessively high [free ADP] in the matrix.

Why Is the Cytosolic ADP Concentration So Low and Stable? Cytosolic [ADP] is in a steady state depending on ATP metabolic hydrolysis and ATP synthase, AAC, and adenylate kinase activity. In standard cells, the regulation of cytosolic [ADP] by adenylate kinase is unlikely, because [MgADP] (9 μM) is far below the K_m of the enzyme for its substrate (250 μM when [Mg^{2+}] is 230 μM) (12). In Mg-deficient cells, the cytosolic concentrations of MgADP and Mg^{2+} were still lower, thus excluding adenylate kinase activity and permitting the accumulation of ADP. Accordingly, AMP remained below the ^{31}P-NMR detection threshold in all NM conditions used, except anoxia. In anoxia, cells transiently accumulate ADP, AMP, and Mg^{2+} (23), indicating that adenylate kinase catalyses nucleotide interconversions according to the processes described by Roberts et al. (19), thus limiting ADP accumulation in some stress situations. In contrast, the K_m of AAC for free ADP (15–40 μM) is sufficient to explain why the cytosolic free ADP concentration stabilizes at approximately 20 μM if ATP synthase is not limiting. Indeed, the absence of ADP and/or AMP accumulation in most physiological situations weakens the hypothesis that ATP synthase activity could be rate-limiting for cell respiration (35).

From a biochemical standpoint, the low cytosolic [ADP] may favor some aspects of cell metabolism, because it promotes the function of MgATP-using enzymes that are competitively inhibited by MgADP, such as nitrogenase (36) and various kinases (37, 38).

Conclusion

The respiration of heterotrophic cells, where most of the demand for ATP is met by mitochondrial oxidative phosphorylation, appears to be controlled principally by the cytosolic release of free ADP and Mg^{2+} from MgATP hydrolysis. The mitochondrial AAC carrier and ATP synthase stabilize the concentration of cytosolic free ADP at a low value that permits precise adjustments of cell respiration to energy demands. The low concentration of Mg^{2+} in the cytosol, together with its high concentration in the matrix, facilitate the import of free ADP in mitochondria. Conversely, Mg^{2+} released in the cytosol binds to the cytosolic free ATP, thereby favoring the export of free ATP from mitochondria. The mechanism permitting the transport of ATP^{4-} from mitochondria at countergradient remains unclear, however. Finally, given the stability of the cytosolic free Mg^{2+} concentration under conditions leading to a fivefold increase in ATP level, and because magnesium is stored mainly in the vacuole, there is a need for further research to characterize the exchange of Mg^{2+} across the vacuolar membrane, to better understand the buffering processes controlling the homeostasis of free Mg^{2+} in the cytosol.

Materials and Methods

Plant Material, Cell Respiration, and Growth Measurements. Heterotrophic sycamore (*Acer pseudoplatanus* L.) cells of cambial origin were grown at 20 °C in Lamport liquid NM (39) as described previously (40). The cell suspensions were maintained in exponential growth by weekly subculturing. Culture aliquots were taken for experiments at day 4 after subculturing.

Cell respiration was measured at 20 °C in the culture medium. Oxygen uptake was measured polarographically with a Clark-type O_2 electrode system (Hansatech). The O_2 concentration in the air-saturated NM at 20 °C was taken as 280 μM. The wet weight of cell samples and the growth of cell suspensions were measured as described previously (40).

When data are reported as mean ± SD, the statistical Student *t* test was applied to the data with a P value ≤ 0.05.

Preparation of Plant Cell Mitochondria and Plastids. Crude mitochondria were isolated from 2 kg of packed cells (41) and purified on a Percoll gradient (42), as described previously. Within 90 min, 2 mL of a thick slurry of mitochondria (0.2 g protein mL^{-1}) was obtained. The intactness and physiological properties of mitochondria were controlled as described previously (42). It was previously shown that NAD might leak out of purified mitochondria, but only slowly and after several hours following the purification procedure (43). To minimize undesired leakage of components initially present in the matrix space, in these experiments we took great care to perform all of the analyses immediately after the final purification step, as was done previously (19, 44). The percentage of mitochondrial intactness measured in five preparations was >90%. Plastids were isolated from cell protoplasts as described previously (20).

^{31}P-NMR Spectroscopy. In vivo and in vitro ^{31}P-NMR spectroscopy on cells and cell extracts was performed using a wide-bore NMR spectrometer (AMX 400; Bruker Instrument). Unless stated otherwise, on in vivo assays, 10 g of sedimented cells was perfused in a 25-mm NMR tube at 20 °C with a well-oxygenated NM maintained at pH 6.0, as described previously (9). The perfusing medium contained the macronutrients normally present in 200 mL of Lamport's medium and no micronutrients, to optimize field homogeneity and further improve the signal-to-noise ratio. Added Pi (50 μM) was sufficient for the cell requirements and yielded only a negligible external Pi peak partially overlapped by vac-Pi.

Quantification of total cell ADP and ATP was done from in vivo and PCA extracts as described previously (9). Considering that an important part of this work is based on the precise in vitro quantification of ATP and ADP, we verified in control experiments on cell samples added with known amounts of nucleotides before extraction process that PCA extraction did not hydrolyze nucleotides.

The measurements of [ATP], [ADP], [MgATP], [MgADP], and [Mg^{2+}] were performed by relating the in vivo chemical shifts (δ) of the γ- and β-phosphorus resonance peaks of ATP and ADP, respectively, to calibration curves obtained in vitro (Fig. S1). The γ-ATP signal was preferred to the β-ATP signal, as well as to measurement of the difference between $\delta_{\beta\text{-ATP}}$ and $\delta_{\alpha\text{-ATP}}$ (13), because it is narrower, thereby allowing more precise measurements and permitting better separation of overlapping peaks. In particular, when the data accumulation time is short (1 h), the precision of measurements from the broader β-ATP signal is poorer despite the greater amplitude of $\delta_{\beta\text{-ATP}}$ (Table S2). After 16 h of data accumulation, the precision is similar, and the results are comparable. In vivo free/Mg-complexed ATP and ADP ratios were calculated as $|\delta - \delta_{max}|/|\delta - \delta_{min}|$, where δ is the chemical shift of the nucleotide measured in vivo and δ_{max} and δ_{min} are the chemical shifts of the nucleotide measured in vitro in the presence of [Mg^{2+}] leading to the highest value on calibration curves (corresponding to 100% Mg-complexed nucleotide) and in the absence of Mg^{2+} (100% free nucleotide), respectively (Fig. S1). In our case, the δ_{max} (−5.30 ppm for ATP and −5.90 ppm for ADP) stabilized at approximately 1.5 mM and 20 mM added $MgSO_4$ for ATP and ADP, respectively.

The δ_{min} depends on different parameters, including pH and ionic strength (45), which may lead to substantial errors in the measurement of free [Mg^{2+}] (46). For this reason, we checked incubation media at different ionic strengths and different nucleotide concentrations to establish the calibration curves.

We chose an incubation medium containing 0.6 mM ATP, 0.15 mM ADP, and 150 mM KNO_3 because it leads to similar [Mg^{2+}] values regardless of whether they are calculated from the $\delta_{\gamma\text{-ATP}}$ or from the $\delta_{\beta\text{-ADP}}$. In addition, the concentrations of nucleotides and KNO_3 in this medium are close to their values in cells. The pH values (7.0, 7.4, and 7.6) are those of purified mitochondria, cytosol, and in vivo mitochondria, respectively. The concentration of Mg^{2+} in the cytosol and in the mitochondrial matrix was calculated from the dissociation constants K_d^{MgATP} = [Mg^{2+}][free ATP]/[MgATP] and K_d^{MgADP} = [Mg^{2+}][free ADP]/[MgADP]. The K_d values were calculated as follows: On a calibration curve, the equilibrium obtained at the midpoint corresponds to a situation in which one-half of the considered nucleotide is free and the other half is complexed with magnesium. At this midpoint, the free magnesium ($K_d^{Mg\text{-nucleotide}}$) corresponds to the difference between added magnesium (reported on the *x*-axis) and complexed magnesium (MgATP + MgADP).

These K_d values are not significant depending on pH in the range tested, and their measured values (K_d^{MgATP} = 35 ± 3 μM and K_d^{MgADP} = 670 ± 50 μM) are consistent with the literature (13, 47). They also do not depend on ATP concentration (between 0.4 and 2 mM) or on the presence of proteins (between 10 and 50 mg BSA mL^{-1}). Indeed, although adding more ATP or protein shifted the calibration curves toward the high *x*-axis values, because higher amounts of magnesium amounts are required to saturate Mg-binding sites, the K_d values remain unchanged. The intrinsic errors on δ and δ_{max} were ± 0.02 ppm, and that on δ_{min} was ± 0.05 ppm. In mitochondria, the main error on free vs. complexed nucleotide measurement originated from the lack of precision on the δ (± 0.1 ppm), owing to broad and noisy peaks.

Measurement of Magnesium. The total magnesium present in water-washed cells and their purified mitochondria was assessed by ICP-MS (Hewlett-Packard 4500 Series; Agilent Technologies, Massy, France), equipped with a Babington nebulizer and a Peltier-cooler double-pass Scott spray chamber.

ACKNOWLEDGMENTS. We thank Eva Pebay-Peyroula and Gérard Brandolin for insightful discussions, Peter Doerner and Jacques Bourguignon for helpful comments on the manuscript, Melissa Conte for English correction, Anne-Marie Boisson for help with cell cultures, and Jean-Luc Le Bail for NMR assistance.

1. Arnold S, Kadenbach B (1999) The intramitochondrial ATP/ADP-ratio controls cytochrome *c* oxidase activity allosterically. *FEBS Lett* 443(2):105–108.
2. Geigenberger P, Riewe D, Fernie AR (2010) The central regulation of plant physiology by adenylates. *Trends Plant Sci* 15(2):98–105.
3. Atkinson DE (1968) The energy charge of the adenylate pool as a regulatory parameter: Interaction with feedback modifiers. *Biochemistry* 7(11):4030–4034.
4. Pradet A, Raymond P (1983) Adenine nucleotide ratios and adenylate energy charge in energy metabolism. *Annu Rev Plant Physiol* 34:199–224.
5. Moore AL (1992) Factors affecting the regulation of mitochondrial respiratory activity. *Molecular, Biochemical and Physiological Aspects of Plant Respiration*, eds Lambers H, van der Plas LHW (SPB Academic Publishing, The Hague, The Netherlands), pp 9–18.
6. Arnold S, Kadenbach B (1997) Cell respiration is controlled by ATP, an allosteric inhibitor of cytochrome-*c* oxidase. *Eur J Biochem* 249(1):350–354.
7. Igamberdiev AU, Kleczkowski LA (2006) Equilibration of adenylates in the mitochondrial intermembrane space maintains respiration and regulates cytosolic metabolism. *J Exp Bot* 57(10):2133–2141.
8. Klingenberg M (2008) The ADP and ATP transport in mitochondria and its carrier. *Biochim Biophys Acta* 1778(10):1978–2021.
9. Pratt J, et al. (2009) Phosphate (Pi) starvation effect on the cytosolic Pi concentration and Pi exchanges across the tonoplast in plant cells: An in vivo 31P-nuclear magnetic resonance study using methylphosphonate as a Pi analog. *Plant Physiol* 151(3): 1646–1657.
10. Rose IA (1968) The state of magnesium in cells as estimated from the adenylate kinase equilibrium. *Proc Natl Acad Sci USA* 61(3):1079–1086.
11. Panov A, Scarpa A (1996) Mg^{2+} control of respiration in isolated rat liver mitochondria. *Biochemistry* 35(39):12849–12856.
12. Igamberdiev AU, Kleczkowski LA (2001) Implications of adenylate kinase-governed equilibrium of adenylates on contents of free magnesium in plant cells and compartments. *Biochem J* 360(Pt 1):225–231.
13. Gupta RK, Yushok WD (1980) Noninvasive ^{31}P NMR probes of free Mg^{2+}, MgATP, and MgADP in intact Ehrlich ascites tumor cells. *Proc Natl Acad Sci USA* 77(5):2487–2491.
14. Bligny R, Douce R (1976) Les mitochondries de cellules végétales isolées. *Physiol Veg* 14(3):499–515.
15. Aubert S, et al. (1996) Ultrastructural and biochemical characterization of autophagy in higher plant cells subjected to carbon deprivation: control by the supply of mitochondria with respiratory substrates. *J Cell Biol* 133(6):1251–1263.
16. Pozueta-Romero J, Frehner M, Viale AM, Akazawa T (1991) Direct transport of ADPglucose by an adenylate translocator is linked to starch biosynthesis in amyloplasts. *Proc Natl Acad Sci USA* 88(13):5769–5773.
17. Bligny R, Foray M-F, Roby C, Douce R (1989) Transport and phosphorylation of choline in higher plant cells: Phosphorus-31 nuclear magnetic resonance studies. *J Biol Chem* 264(9):4888–4895.
18. Aubert S, Gout E, Bligny R, Douce R (1994) Multiple effects of glycerol on plant cell metabolism: Phosphorus-31 nuclear magnetic resonance studies. *J Biol Chem* 269(34): 21420–21427.
19. Roberts J, Aubert S, Gout E, Bligny R, Douce R (1997) Cooperation and competition between adenylate kinase, nucleoside diphosphokinase, electron transport, and ATP synthase in plant mitochondria studied by ^{31}P-nuclear magnetic resonance. *Plant Physiol* 113(1):191–199.
20. Macherel D, Kobayashi H, Akazawa T, Kawano S, Kuroiwa T (1985) Amyloplast nucleoids in sycamore cells and presence in amyloplast DNA of homologous sequences to chloroplast genes. *Biochem Biophys Res Commun* 133(1):140–146.
21. Vicente JAF, Madeira VMC, Vercesi AE (2004) Regulation by magnesium of potato tuber mitochondrial respiratory activities. *J Bioenerg Biomembr* 36(6):525–531.
22. Gupta RK, Benovic JL, Rose ZB (1978) The determination of the free magnesium level in the human red blood cell by 31P NMR. *J Biol Chem* 253(17):6172–6176.
23. Gout E, Boisson A, Aubert S, Douce R, Bligny R (2001) Origin of the cytoplasmic pH changes during anaerobic stress in higher plant cells: Carbon-13 and phosphorous-31 nuclear magnetic resonance studies. *Plant Physiol* 125(2):912–925.
24. Marschner H (1995) *Mineral Nutrition of Higher Plants* (Academic Press, San Diego, CA), 2nd Ed, pp 278–282.
25. Shaul O (2002) Magnesium transport and function in plants: The tip of the iceberg. *Biometals* 15(3):309–323.
26. Aubert S, Juge C, Boisson A-M, Gout E, Bligny R (2007) Metabolic processes sustaining the reviviscence of lichen *Xanthoria elegans* (Link) in high mountain environments. *Planta* 226(5):1287–1297.
27. Saint-Ges V, Roby C, Bligny R, Pradet A, Douce R (1991) Kinetic studies of the variations of cytoplasmic pH, nucleotide triphosphates (^{31}P-NMR) and lactate during normoxic and anoxic transitions in maize root tips. *Eur J Biochem* 200(2):477–482.
28. Jobic C, et al. (2007) Metabolic processes and carbon nutrient exchanges between host and pathogen sustain the disease development during sunflower infection by *Sclerotinia sclerotiorum*. *Planta* 226(1):251–265.
29. Klingenberg M (1980) The ADP-ATP translocation in mitochondria, a membrane potential controlled transport. *J Membr Biol* 56(2):97–105.
30. Dehez F, Pebay-Peyroula E, Chipot C (2008) Binding of ADP in the mitochondrial ADP/ATP carrier is driven by an electrostatic funnel. *J Am Chem Soc* 130(38):12725–12733.
31. Knirsch M, Gawaz MP, Klingenberg M (1989) The isolation and reconstitution of the ADP/ATP carrier from wild-type *Saccharomyces cerevisiae*: Identification of primarily one type (AAC-2). *FEBS Lett* 244(2):427–432.
32. Haferkamp I, Hackstein JHP, Voncken FGJ, Schmit G, Tjaden J (2002) Functional integration of mitochondrial and hydrogenosomal ADP/ATP carriers in the *Escherichia coli* membrane reveals different biochemical characteristics for plants, mammals and anaerobic chytrids. *Eur J Biochem* 269(13):3172–3181.
33. Cieslar JH, Dobson GP (2000) Free [ADP] and aerobic muscle work follow at least second-order kinetics in rat gastrocnemius *in vivo*. *J Biol Chem* 275(9):6129–6134.
34. Schünemann D, Borchert S, Flügge U-I, Heldt HW (1993) ADP/ATP translocator from pea root plastids: Comparison with translocators from spinach chloroplasts and pea leaf mitochondria. *Plant Physiol* 103(1):131–137.
35. Stubbs M, Vignais PV, Krebs HA (1978) Is the adenine nucleotide translocator rate-limiting for oxidative phosphorylation? *Biochem J* 172(2):333–342.
36. Cordewener J, Haaker H, Van Ewijk P, Veeger C (1985) Properties of the MgATP- and MgADP-binding sites on the Fe protein of nitrogenase from *Azotobacter vinelandii*. *Eur J Biochem* 148(3):499–508.
37. Renz A, Stitt M (1993) Substrate specificity and product inhibition of different forms of fructokinases and hexokinases in developing potato tubers. *Planta* 190(2):166–175.
38. Nishimasu H, Fushinobu S, Shoun H, Wakagi T (2007) Crystal structures of an ATP-dependent hexokinase with broad substrate specificity from the hyperthermophilic archaeon *Sulfolobus tokodaii*. *J Biol Chem* 282(13):9923–9931.
39. Lamport DTA (1964) Cell suspension cultures of higher plants: Isolation and growth energetics. *Exp Cell Res* 33:195–206.
40. Bligny R, Leguay J-J (1987) Techniques of cell suspension culture. *Methods Enzymol* 148:3–16.
41. Bligny R, Douce R (1977) Mitochondria of isolated plant cells (*Acer pseudoplatanus* L.), II: Copper deficiency effects on cytochrome *C* oxidase and oxygen uptake. *Plant Physiol* 60(5):675–679.
42. Neuburger M, Journet EP, Bligny R, Carde J-P, Douce R (1982) Purification of plant mitochondria by isopycnic centrifugation in density gradients of Percoll. *Arch Biochem Biophys* 217(1):312–323.
43. Neuburger M, Douce R (1983) Slow passive diffusion of NAD^+ between intact isolated plant mitochondria and suspending medium. *Biochem J* 216(2):443–450.
44. Aubert S, et al. (2001) Contribution of glutamate dehydrogenase to mitochondrial glutamate metabolism studied by $^{(13)}C$ and $^{(31)}P$ nuclear magnetic resonance. *J Exp Bot* 52(354):37–45.
45. Lundberg P, Harmsen E, Ho C, Vogel HJ (1990) Nuclear magnetic resonance studies of cellular metabolism. *Anal Biochem* 191(2):193–222.
46. Mosher TJ, Williams GD, Doumen C, LaNoue KF, Smith MB (1992) Error in the calibration of the MgATP chemical-shift limit: Effects on the determination of free magnesium by ^{31}P NMR spectroscopy. *Magn Reson Med* 24(1):163–169.
47. Williams GD, Mosher TJ, Smith MB (1993) Simultaneous determination of intracellular magnesium and pH from the three ^{31}P NMR chemical shifts of ATP. *Anal Biochem* 214(2):458–467.